International Journal of Biological Macromolecules 250 (2023) 126009

Contents lists available at ScienceDirect

International Journal of Biological Macromolecules

journal homepage: www.elsevier.com/locate/ijbiomac

Glycosylation of polyphenolic compounds: Design of a self-sufficient biocatalyst by co-immobilization of a glycosyltransferase, a sucrose synthase and the cofactor UDP

Lara Trobo-Maseda [a], María Romero-Fernandez [a], José M. Guisan [a,*], Javier Rocha-Martin [b,*]

[a] Department of Biocatalysis, Institute of Catalysis and Petrochemistry (ICP) CSIC, Campus UAM, Cantoblanco, 28049 Madrid, Spain
[b] Department of Biochemistry and Molecular Biology, Faculty of Biological Sciences, Complutense University of Madrid, 28040 Madrid, Spain

ARTICLE INFO

Keywords:
Sucrose synthase
Glycosyltransferase
Co-immobilization
Colocalization
Glycobiotechnology
Self-sufficient biocatalyst

ABSTRACT

Glycosyltransferases catalyze the regioselective glycosylation of polyphenolic compounds, increasing their solubility without altering their antioxidant properties. Leloir-type glycosyltransferases require UDP-glucose as a cofactor to glycosylate a hydroxyl of the polyphenol, which is expensive and unstable. To simplify these processes for industrial implementation, the preparation of self-sufficient heterogeneous biocatalysts is needed. In this study, a glycosyltransferase and a sucrose synthase (as an UDP-regenerating enzyme) were *co*-immobilized onto porous agarose-based supports coated with polycationic polymers: polyethylenimine and polyallylamine. In addition, the UDP cofactor was strongly ionically adsorbed and co-immobilized with the enzymes, eliminating the need to add it separately. Thus, the optimal self-sufficient heterogeneous biocatalyst was able to catalyze the glycosylation of three polyphenolic compounds (piceid, phloretin and quercetin) with *in situ* regeneration of the UDP-glucose, allowing multiple consecutive reaction cycles without the addition of exogenous cofactor. A TTN value of 50 (theoretical maximum) was obtained in the reaction of piceid glycosylation, after 5 reaction cycles, using the self-sufficient biocatalyst based on an improved sucrose synthase variant. This result was 5-fold higher than the obtained using soluble cofactor and the co-immobilized enzymes, and much higher than those reported in the literature for similar processes.

1. Introduction

The enzymatic synthesis of glycosides, products of glycosylation reactions, has received increasing attention in organic synthesis with the aim of replacing or reducing the use of dangerous, time-consuming and costly chemical synthesis methodologies [1–3]. Glycosides include natural oligosaccharides and polysaccharides in free form or bound to other biomolecules, such as lipids and proteins, with application in the food or feed industries ingredients [4], glycosylated molecules of medical interest (including protein biopharmaceuticals) [5–7], small glycosylated molecules as a major component of cosmetic products [8], in flavors and fragrances [9,10]. The search for new glycosyltransferases (GTs) (EC 2.4.1) with improved tolerance to donor and acceptor substrates plays an important key to produce various glyco-functionalized natural products in an environmentally friendly and cost-effective way [11,12].

GTs are stereoselective enzymes primarily involved in natural product glycosylation, which is well known to change the physical, chemical and biological properties of small molecules [13]. GTs catalyze the transfer of a carbohydrate acceptor from a nucleotide donor of activated sugars with high selectivity and efficiency, enabling the stereo- and regioselective extension and branching of large glycans and glycoconjugates. Leloir GTs utilize carbohydrates linked to a nucleotide diphosphate (NDP) with an α-linked glycosidic bond [14]. However, the use of Leloir GTs involves the exogenous addition of UDP-glucose as a cofactor, which implies some economic constraints on the feasibility of the process on an industrial scale. Thus, the vast majority of enzymatic processes applied to the synthesis of glycosylated bioactive compounds incorporate cofactor recycling systems [15–17].

Sucrose synthase (SuSy, EC 2.4.1.13) catalyzes the reversible conversion of NDP and sucrose into NDP-glucose and fructose [18]. Thus, SuSy is one of the most promising candidates to solve the supply of NDP-glucose for the production of high-cost nucleotide sugars from the cheap and abundant substrate sucrose [19]. Therefore, GTs can be coupled to

* Corresponding authors.
E-mail addresses: jmguisan@icp.csic.es (J.M. Guisan), javrocha@ucm.es (J. Rocha-Martin).

https://doi.org/10.1016/j.ijbiomac.2023.126009
Received 17 February 2023; Received in revised form 29 June 2023; Accepted 25 July 2023
Available online 1 August 2023

SuSys to create an enzymatic cascade that efficiently and economically catalyzes the selective glycosylation of a wide variety of apolar compounds with *in situ* regeneration of UDP-glucose. Currently, cascades coupling GT and SuSy enzymes for regeneration of nucleotide sugars and optimization of the production of these proteins have been explored [15,20–22]. However, the application of Leloir GTs in a multienzyme sugar coupling processes is challenging from a process design point of view. The difficult production of recombinant Leloir GTs (microbial or plant), their low stability, the limited availability of nucleotide sugar donors, the high costs and low stability of nucleotides, limit the application of nucleotide-dependent Leloir GTs in the industry [14,23,24]. Therefore, the development of robust glycosylation methods is a goal of central importance in this field.

The immobilization of multienzyme systems on solid materials is an effective strategy for establishing *in vitro* multienzyme catalytic systems. This technology is receiving an increasing interest for the construction of biocatalytic cascades with biotechnological applications in industry [25,26]. The control of the spatial organization of multienzyme systems within porous materials is essential to improve the performance of the bioprocess providing higher robustness, yield and productivity [21,27,28], and can be achieved by modulating the immobilization rate [29]. In addition, the use of self-sufficient biocatalysts, where enzymes and cofactors are co-immobilized on the same solid material, avoids the need to add exogenous cofactor during several reaction cycles [30–33]. A simple way to fabricate these biocatalysts is to adsorb the diphosphorylated cofactors onto polycationic solid supports on which the enzymes are previously immobilized. Such adsorption is dynamic and makes possible that some phosphorylated cofactors remain adsorbed on the positively charged solid support, while only a small percentage is released and available for the active site of the enzyme molecules. Therefore, the cofactors can be recycled inside the porous particles and both cofactor and enzymes can be re-used for several operational cycles [30,33].

Considering the current limitations of glycosylation processes, we have decided to fabricate a robust self-sufficient bi-enzymatic heterogeneous biocatalyst for the glycosylation of different polyphenols compounds. For this purpose, we first evaluated the immobilization and stabilization of UDP cofactor on three different anion exchangers based on agarose beads: DEAE (diethylaminoethyl)-Sepharose, polyethyleneimine-agarose (PEI—Ag) and polyallylamine-agarose (PAA—Ag). After, a SuSy from *Acidithiobacillus caldus* (SuSyAc), a GT from *Malus domestica* (UGT71A15, UGT) and UDP cofactor were *co*-immobilized on the polycationic supports. Although it has been reported that plant SuSys preferentially use UDP as the main nucleotide substrate and bacterial SuSy ADP [18], we used the bacterial SuSyAc because of its higher thermostability and high expression yield. In addition, for the preparation of the optimized self-sufficient heterogeneous biocatalyst, we used a SuSyAc double mutant (L637M-T640V, $SuSyAc_{mut}$) with a 60-fold reduced K_m for UDP to enhance UDP-glucose recycling significantly [34]. Thus, the recycling efficiency of UDP-glucose on the piceid glycosylation catalyzed by the different co-immobilized preparations was compared using soluble UDP and co-immobilized UDP. Finally, the optimized self-sufficient biocatalyst was also used in the glycosylation reaction of quercetin and phloretin. These three polyphenolic compounds have positive effects for human health, and its glycosylation may lead to increase their solubility, stability and bioavailability [35–40]. The optimized self-sufficient heterogeneous biocatalyst was able to regenerate and retain the UDP cofactor in the polycationic porous support for several operational batch-cycles without the addition of exogenous UDP to achieve the corresponding glycosylated compounds in 100% yield.

2. Experimental section

2.1. Materials

Polyallylamine (PAA, Mw ~ 17.5 kDa), polyethyleneimine (PEI, Mw ~ 25 kDa), 4-(2-hydroxyethyl)piperazine-1-ethanesulfonic acid (HEPES), tris(hydroxymethyl)aminomethane (TRIS), 3-(N-morpholino) propanesulfonic acid (MOPS), D-fructose, sucrose, bovine serum albumin (BSA), pyruvate kinase/lactic dehydrogenase (PK/LD) enzymes from rabbit muscle, phospho-enol pyruvate (PEP), magnesium chloride hexahydrate, 1,4-butanediol diglycidyl ether (BDGE), epichlorohydrin (EPI), tetranbutylammonium bromide (TBAB), phloretin (99% purity), phloridzin (98% purity), quercetin (95% purity), quercetin 3-glucoside (98% purity) and quercetin 7-glucoside (98% purity) were purchased from Sigma-Aldrich Co. (St. Louis, IL, USA). Uridine 5′-diphosphoglucose disodium salt (UDP-glucose), uridine diphosphate (UDP), piceid (95% purity) and reduced β-nicotinamide adenine dinucleotide disodium salt (NADH) were obtained from Carbosynth (Berkshire, UK). Standard 4% beads crosslinked (BCL) agarose (50–100 μM size particle) were purchased from Agarose Beads Technology (Madrid, Spain). Diethylaminoethyl (DEAE)-Sepharose was purchased from GE Healthcare (Uppsala, Sweden). All reagents were of analytical grade.

2.2. Methods

2.2.1. Enzyme production and purification

N-terminal *strep*-tag UGT71A15 from *Malus domestica* (UGT; GenBank: DQ103712) and N-terminal His_6-tag SuSy from *Acidithiobacillus caldus* (SuSyAc; UniProtKB: A0A059ZV61) overexpressed in *Escherichia coli* were produced and purified as published elsewhere [41,42]. SuSyAc variant ($SuSyAc_{mut}$; L637M-T640V double mutant) was constitutively expressed in *E. coli* BL21 (DE3), and purified by Ni–NTA chromatography according to the protocol established by Diricks et al. [42]. As a final purification step, the enzymes were dialyzed overnight against 10 mM sodium phosphate buffer at pH 7.0. Protein concentrations were determined using a BCA Protein Assay Kit from Pierce (Rockford, IL, USA).

2.2.2. Enzyme assays

The activity of free and immobilized SuSyAc (wild type or variant) preparations was spectrophotometrically measured using a continuous enzymatic assay, where the production of the UDP was determined according to the previously described enzyme-coupling method (pyruvate kinase/lactate dehydrogenase system) [43]. Briefly, the reaction mixture contained 1 mL of 1 M HEPES at pH 8.5, 2 U of pyruvate kinase, 2 U of lactate dehydrogenase, 200 μL of bovine serum albumin 1.3% (*w*/*v*), 200 μL of 130 mM $MnCl_2$, 120 μL of 7 mM phosphoenolpyruvate, 60 μL of 6 mM NADH, 60 μL of 50 mM UDP-glucose, 100 μL of 1 M fructose and enzyme at an appropriate concentration. The final volume of the assay was 2 mL. The formation of UDP was followed spectrophotometrically at 340 nm and 42 °C in V-730 spectrophotometer from JASCO Analitica Spain S.L. (Madrid, Spain) equipped with a thermostatically controlled cell and continuous magnetic stirring. One unit of SuSy activity (U) was defined as the amount of enzyme that released 1 μmol of UDP per minute under given conditions and considering an $\varepsilon = 6220$ M^{-1} cm^{-1} at 340 nm.

The kinetic parameters of the SuSyAc and $SuSyAc_{mut}$ were compared using the bicinchoninic acid (BCA) method, which detect the fructose released by SuSy during the cleavage of sucrose. Reagent was prepared by combining 23 parts of a solution containing 1.5 $g{\cdot}L^{-1}$ of 4,4′-dicarboxy-2,2′-biquinoline dipotassium salt and 62.3 $g{\cdot}L^{-1}$ anhydrous Na_2CO_3, 1 part of a solution composed of 23 $g{\cdot}L^{-1}$ aspartic acid, 33 $g{\cdot}L^{-1}$ anhydrous Na_2CO_3 and 7.3 $g{\cdot}L^{-1}$ $CuSO_4$ and 6 parts ethanol. Then, the 96-well plate was covered with a plastic foil and incubated at 70 °C for 30 min. After cooling to room temperature, the absorbance was measured. The resulting OD values are proportional to the amount of

fructose present in the sample. Kinetic parameters for UDP were determined with 200 mM sucrose in 100 mM MOPS at pH 7.0 and 60 °C [34]. Sample (25 μL) was mixed with 150 μL of assay solution. After the addition of enzyme, samples were taken during 10 min and the absorbance was determined at 540 nm. One unit of SuSy activity is defined as the amount of enzyme that released 1 μmol of fructose min^{-1} under the specified conditions. Due to the low protein concentrations (from 0.5 to 2 $mg{\cdot}L^{-1}$), no significant background signal was observed. Apparent K_m and V_{max} values were estimated by non-linear regression of the Michaelis–Menten equation using Sigma Plot 11.0.

For determination of the soluble and immobilized UGT activity, the reaction of glycosylation of *p*-nitrophenol was performed as previously described [21]. The assay was performed in 2 mL scale, containing 50 mM HEPES pH 8.0, 0.1 mM *p*-nitrophenol, 2 mM UDP-glucose and 100 μg/mL of UGT. The decrease in absorbance at 420 nm and 30 °C was recorded in a spectrophotometer equipped with a thermostatically controlled cell and continuous magnetic stirring. One activity unit (U) of UGT was defined as the amount of enzyme that glycosylated 1 μmol of *p*-nitrophenol per minute under given conditions.

2.2.3. Activation of agarose based supports

2.2.3.1. Glyoxyl-agarose support (G-Ag). The G-Ag support was prepared according to the literature using agarose 4 BCL [44].

2.2.3.2. PEI-agarose support (PEI-Ag). PEI-Ag support was prepared from fully activated G-Ag using agarose 4BCL and covered with PEI polymer (Mw ~ 25 kDa) as previously described [45].

2.2.3.3. PAA-agarose support (PAA-Ag). The procedure to fabricate this support is very similar to the PEI-Ag's procedure support [45]. Briefly, the G-Ag support was dissolved in 100 mM sodium bicarbonate buffer at pH 10.0 containing 0.2 g PAA (Mw ~ 17.5 kDa)/mL support. The mixture was incubated under gently stirring during 3 h at 25 °C, and then reduced by adding 10 mg/mL of solid sodium borohydride. The suspension was incubated for 2 h at 25 °C under gently stirring. The support was then washed sequentially with 100 mM sodium acetate at pH 4.0, 100 mM sodium borate at pH 9.0, 1 M NaCl and finally with distilled water in excess to remove any PAA molecules adsorbed on the support.

2.2.4. Immobilization of UDP and enzymes

Enzymes and cofactor were immobilized on different agarose-activated supports at the indicated pH and temperature under gently stirring conditions. At different times during the process, samples of the control solution (enzyme incubated under immobilization conditions), supernatant and suspension were withdrawn to determine their catalytic activities, using the enzyme assays described above.

Immobilization yield was defined as the amount of enzyme attached to the support and calculated as the ratio between the activity in the supernatant compared to the activity in the control. Expressed activity was defined as the final activity of the biocatalyst and calculated as the ratio of the activity in the final suspension after the immobilization process and the activity of the control.

$$\text{Immobilization yield } (\%) = \left(1 - \frac{\text{Final supernatant activity } \left(U/mL\right)}{\text{Initial activity } \left(U/mL\right)}\right) \bullet 100$$

$$\text{Expressed activity } (\%) = \left(\frac{\text{Suspension activity } \left(U/mL\right).\text{Yield}}{\text{Initial activity } \left(U/mL\right)}\right) \bullet 100$$

2.2.4.1. Immobilization of UDP cofactor. The ion exchange immobilization of the phosphorylated cofactor UDP was achieved incubating 0.1 g of the polycationic support (DEAE-Sepharose, PEI-Ag and PAA—Ag) in 10 mL of a solution containing 1 mM UDP dissolved in 0.1 M HEPES at pH 7.0. The suspension was kept under orbital agitation for 2 h at 4 °C. Finally, the suspension was vacuum filtered and washed with 10 volumes of 10 mM sodium phosphate at pH 7.0. The optimization of the immobilization of UDP on PEI-Ag was performed under the indicated buffer (HEPES or Tris-HCl) and concentration (5, 25, 50 or 100 mM) at pH 7.0. Concentration of the immobilized UDP was determined by measuring the absorbance of the supernatants after the adsorption process and after each wash at a wavelength of 262 nm [33].

2.2.4.2. Determination of the cofactor stability. The different immobilized cofactor preparations were incubated in 10 mM sodium phosphate buffer at pH 7.0 and 30 °C. Samples of the suspensions (support plus UDP cofactor) were withdrawn at different time points and the stability of the different immobilized UDP preparations was evaluated by monitoring changes in the absorbance at 262 nm as a function of incubation time under desired conditions.

2.2.4.3. Binding strength of UDP to polycationic supports. The immobilized UDP preparations were incubated 1/10 (*w/v*) in growing concentrations of NaCl (0–350 mM) in 5 mM sodium bicarbonate at pH 9.0 and 25 °C. Activity of suspensions and supernatant was determined as described above. Supernatant samples were taken after 15 min of incubation in the presence of different concentrations of ionic strength. A reference solution with soluble cofactor was subjected to the same treatment to detect any possible artefacts of NaCl on the cofactor measurements. The concentration of the UDP was determined by measuring the absorbance at 262 nm.

2.2.4.4. Co-immobilization of SuSyAc/SuSyAc$_{mut}$ and UGT on PEI-Ag (SuSyAc-UGT-PEI-Ag and SuSyAc$_{mut}$-UGT-PEI-Ag biocatalysts). The co-immobilization of purified SuSyAc or SuSyAc$_{mut}$ and UGT enzymes on PEI-Ag was performed as described in bibliography [21]. The co-immobilization was performed in two steps. First, 1 g of the PEI-Ag support was suspended 1:10 (*w/v*) in the enzyme solution, composed by 1 mg of SuSyAc or SuSyAc$_{mut}$ dissolved in 25 mM sodium phosphate buffer at pH 7.0. Secondly, a solution containing 10 mg of UGT was added to the previous mixture. Finally, the co-immobilized biocatalysts were vacuum filtered and washed with 10 volumes of 10 mM sodium phosphate buffer at pH 7.0.

2.2.4.5. Co-immobilization of SuSyAc and UGT on PAA-Ag (SuSyAc-UGT-PAA-Ag biocatalyst). The immobilization was conducted by adding 1 g of PAA-Ag support to 10 mL of 25 mM phosphate buffer at pH 7.0 containing 1 mg of SuSyAc and 10 mg of UGT. This suspension was incubated for 12 h at 4 °C under mild stirring. When the immobilization was completed, the co-immobilized biocatalyst was vacuum filtered and washed with 10 volumes of 10 mM sodium phosphate buffer at pH 7.0.

2.2.4.6. Preparation of the self-sufficient heterogeneous biocatalysts: Co-immobilization of UDP on the polycationic supports. Once SuSyAc and UGT were immobilized on PEI-Ag or PAA—Ag, 1 g of the heterogeneous biocatalyst was incubated with a freshly prepared solution of 50 μM of UDP in 6.66 mL of 50 mM Tris-HCl buffer at pH 7.0 for 2 h at 4 °C under orbital shaking. Finally, the heterogeneous biocatalyst was filtered and washed with 10 volumes of 10 mM sodium phosphate buffer at pH 7.0. The concentration of the immobilized UDP was calculated by measuring the absorbance of the supernatants after the immobilization process and after each wash at a wavelength of 262 nm.

2.2.5. Glycosylation of piceid, phloretin and quercetin catalyzed by the self-sufficient heterogeneous biocatalyst SuSyAc$_{mut}$-UGT-PEI-Ag

The glycosylation of piceid reactions with *in situ* UDP-glucose

regeneration were performed with a ratio of 1:7 (w of co-immobilized biocatalyst/v of the reaction mixture). The reaction mixture was composed of 500 μM piceid dissolved in 10% DMSO in the indicated buffer (50 mM HEPES or Tris-HCl) and 100 mM of sucrose. For phloretin and quercetin glycosylation, the substrate was dissolved in the presence of 25% DMSO. For piceid and phloretin, all the reaction mixture was adjusted to pH 7.0. In the case of quercetin glycosylation, the pH was adjusted to 8.0. The reaction was triggered by adding 50 μM of exogenous UDP or immobilized UDP (0.33 $\mu mol_{UDP} \times g^{-1}$ of support). Reactions were incubated or 16 h and 30 °C under orbital shaking (80 rpm) and then stopped by vacuum filtration. The co-immobilized biocatalyst was washed with 5 volumes of 10 mM sodium phosphate pH 7.0 after completion of the reaction and reused for the following cycles. Fresh substrate was added to start a new reaction cycle (without exogenous UDP addition). Samples were withdrawn from the reaction bulk at different time points (but never removing >5% of the total reaction volume) and filtered. Finally, the samples were analyzed by Ion-Pair Reversed-Phase High Performance Liquid Chromatography (IP-RP-HPLC) and RP-HPLC coupled to electrospray ionization quadropole time-of-flight mass spectrometry when is indicated. The cofactor total turnover number per cycle (TTN) was calculated as: glycosylated product (mol) detected after batch reaction/UDP (mol) added in the reaction mixture or co-immobilized with the enzymes. The accumulated TTN values mean the sum of all TTN values after each reaction cycle.

2.2.6. Ion-pair reversed-phase high performance liquid chromatography (IP-RP-HPLC)-based determination of glucosides and uridine-derivates

Resveratrol-glucosides and uridine-derivates (UMP, UDP and UDP-glucose) were analyzed in a single run as previously published [41]. The products of the glycosylation reaction of phloretin was analized by HPLC according to the method proposed by Bungaruang *et al* [1]. The quercetin and its glucosides were analyzed as previously reported by Lepak *et al* [41] with some modifications. Briefly, 20 μL of the supernatant were used for analysis on a Spectra Physic SP 100 pump coupled with a UV6000LP photodiode array detector equipped with a C18 column (Kinetex 5 μm C18 100 Å column 50 × 4.6 mm from Phenomenex, USA). The column was thermostatically controlled at 25 °C and the separation was monitored by UV detection at 280 nm. Separation of quercetin and its glycosides was achieved by following method at a constant flow rate of 2.0 mL/min using the gradient: from 0 to 5 min the acetonitrile/TBAB gradient was 40–60%; from 5 to 8 min 50–50% and from 8 to 16 min isocratic flow at 50–50%.

2.2.7. RP-HPLC coupled to electrospray ionization quadropole time-of-flight mass spectrometry (RP-HPLC–ESI-Q-TOF-MS)

The determination of the exact mass of the compounds obtained after the glycosylation reaction was performed by the previously reported method [21]. The use of broadband collision-induced dissociation (bbCID) was applied to the glycosylated reaction products using a high-resolution Bruker maXis II mass spectrometer. In bbCID precursor and product ion spectra were obtained by alternating low and high collision energy. Thus, a characteristic fragmentation fingerprint of the products of each glycosylation reaction was obtained to facilitate their qualitative and quantitative analysis. Briefly, an Agilent Model 1100 with an extended C18 column (Agilent Extend-C18 column 5 μm, 150 × 4.6 mm, Agilent, USA) coupled to an ESI-QTOF MAXIS II (Bruker USA) mass detector was used. Phase A was formed by acetonitrile and 0.1% formic acid and phase B was composed of water and 0.1% formic acid. The gradient was from 0 to 15 min, from 10 to 80% of phase A. From 15 to 20 min, isocratic flow 80% of phase A. From 20 to 25 min, from 80 to 10% of phase A. The temperature of the column was set at 40 °C and flow rate at 1 mL/min.

Data acquisition was performed with Compass HyStar 3.2 and data treatment with Dissect algorithm of Data Analysis 4.4 (Bruker). To determine the molecular formula of each detected compound from its exact and isotopic pattern the SmartFormula tool was used and compared with previously reported glycoside compounds. Compound Crawler was applied to generate putative identifications.

3. Results and discussion

3.1. Immobilization of UDP on cationic agarose-based supports

An enzymatic system to carry out the selective glycosylation of polyphenolic compounds catalyzed by a GT with *in situ* UDP-glucose regeneration mediated by a SuSy was designed. Inspired by the elegant work of Velasco-Lozano and co-workers [33], we initially tested different cationic supports for the immobilization of UDP cofactor to develop a self-sufficient heterogeneous biocatalyst.

The immobilization of negatively-charged phosphorylated cofactors, such as PLP, FAD^+, and NAD^+, takes place by adsorption onto positively-charged supports like cationic polymer-modified supports [31,33,46], and avoids the exogenous addition of cofactor for several reaction cycles. This type of immobilization is reversible, and therefore, it enables an association/dissociation equilibrium from the solid surface. Based on previous findings [21], we hypothesized that the UDP cofactor could also interact with cationic-activated immobilization supports. Immobilizing this cofactor onto the same solid support as UGT and SuSyAc enzymes would provide the additional benefit of a simpler glycosylation process. In this way, we evaluated the immobilization of the UDP cofactor on three positively-charged activated supports: PEI—Ag, PAA-Ag and DEAE-Sepharose.

UDP immobilization studies were carried out on three different cationic polymer-modified supports. By offering 100 $\mu mol_{UDP} \times g^{-1}$ of support at low buffer concentration (100 mM HEPES at pH 7.0), the PAA—Ag, PEI-Ag and DEAE-Sepharose supports adsorbed 98%, 96% and 60% of the offered cofactor, respectively (Table S1). These results are in agreement with those previously reported for phosphorylated cofactors such as NAD^+ (17.5 $\mu mol^+_{NAD} \times g^{-1}$ of support), PLP (83.3 $\mu mol_{PLP} \times g^{-1}$ of support) and FAD (46.1 $\mu mol_{FAD} \times g^{-1}$ of support) [33]. We would like to point out that we also carried out an evaluation of the adsorption of UDP on the polycationic supports at pH 4.0. However, we did not observe any notable variations in the UDP adsorption profiles between the two pH conditions (results not shown).

The efficiency of the UDP immobilization on the PEI-Ag support was evaluated using two different buffers (HEPES and Tris-HCl) and at different concentrations (5–100 mM) (Fig. S1). HEPES was the buffer selected in the glycosylation reactions previously carried out by Lepak et al. [41]. However, we hypothesized that the presence of a sulfonic group in its structure could hinder the binding of the cofactor to the cationic support. For this reason, Tris-HCl buffer was also evaluated. In both cases, >80% cofactor immobilization was achieved, except when using 100 mM buffer concentrations. When Tris-HCl was used as immobilization buffer, there was a slight increase in the amount of immobilized UDP. In view of these results, a Tris-HCl concentration of 25–50 mM was selected as the appropriate buffer for UDP immobilization.

3.2. Binding strength of UDP to the cationic supports

The binding strength of the UDP cofactor to the different cationic supports was also evaluated. As shown in Fig. 1, the ionic strength necessary to desorb the UDP immobilized on PAA-Ag at pH 9.0 was higher than in the case of the UDP adsorbed to PEI-Ag and DEAE-Sepharose. The results showed that primary amine groups promote a more intense adsorption than secondary or tertiary amine groups, as PAA-Ag (having only primary amine groups) promotes a higher percentage of UDP immobilization than PEI-Ag (which has a mixture of primary, secondary and tertiary amine groups in an approximate ratio of 25/50/25) and DEAE-Sepharose (a weak anion exchanger containing diethylaminoethyl groups with 100% tertiary amine groups) [47–49]. It should be noted that the cofactor was retained more tightly at pH values

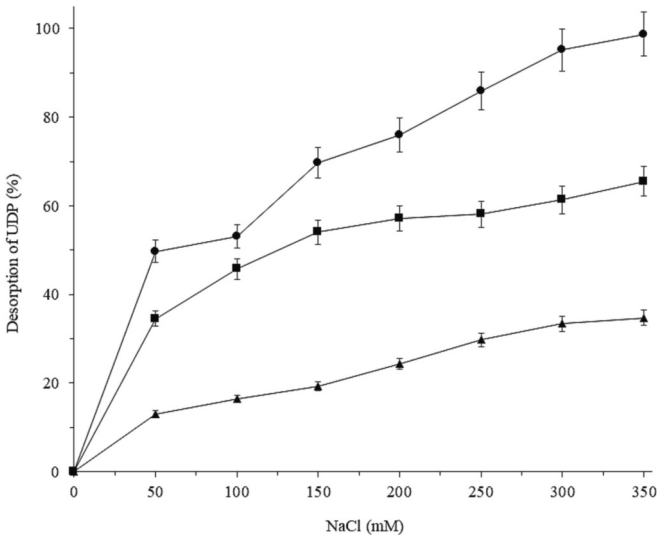

Fig. 1. Desorption of immobilized UDP on different polycationic-modified supports using increasing concentrations of NaCl at pH 9.0 and 30 °C. Symbols: (■) UDP immobilized on PEI-Ag (▲) UDP immobilized on PAA-Ag and (●) UDP immobilized on DEAE-Sepharose.

close to 6 than 9 in all the supports (results not shown). This observation aligns with the study conducted by Suh and co-workers [48], who demonstrated that as pH increases, the fraction of deprotonated nitrogens increases in both PEI and PAA. Thus, the interaction between polyamines and the UDP is favored at pH values ≤7.0. This preference arises from the presence of a higher fraction of protonated nitrogens in the polyamines which enhances their interaction with the negatively charged diphosphate group of the UDP.

Focusing on the two positively-charged supports that bind UDP with the higher intensity, PEI-Ag and PAA—Ag, the apparent dissociation constant (K_d^{app}) was determined. K_d^{app} is defined as the ionic interaction of one molecule of UDP with one positively amine group of the cationic support. The K_d^{app} for UDP-PEI-Ag equilibrium was 6.9-fold lower than for UDP-PAA-Ag (Table S1). In addition, the K_d^{app} obtained for the UDP-PEI-Ag interaction was 3 and 11-fold lower than that obtained for the NAD^+-PEI-Ag and FAD^+-PEI-Ag interaction, respectively, as described previously [33]. However, despite these observed differences, both cationic supports retained 99% of the cofactor after five washing cycles with 10 mM phosphate buffer at pH 7.0 (Table S2). This pH value has been established as optimal for both glycosylation reactions and the stability of the enzymes that are subsequently co-immobilized with the cofactor on the same support. The high retention of the cofactor on the solid phase after multiple washing cycles serves as a strong indication of its low leaching. This result is particularly encouraging, as it demonstrates the robustness and durability of the immobilization system, ensuring minimal loss of UDP from the solid phase.

3.3. Stability of the immobilized cofactor

Finally, the stability of the immobilized cofactor on the three cationic supports was compared with the soluble cofactor at pH 7.0 and 30 °C (optimal reaction conditions) (Fig. 2). The UDP adsorbed on PAA—Ag, PEI-Ag and DEAE-Sepharose was 12, 6 and 2-fold more stable than the free cofactor, respectively. These results could be explained by the higher density of primary amine groups in PAA polymer compared to PEI, and DEAE-Sepharose, which has a stronger binding strength than secondary or tertiary amino groups [50]. It seems that one possible cause of UDP inactivation, the rupture of the phosphodiester bond, is much more limited when immobilizing UDP on PAA—Ag, as the two anions of 2 phosphates from UDP can simultaneously bind to two primary aminos of the polymer hindering its cleavage.

3.4. Evaluation and comparison of piceid glycosylation reactions using exogenous UDP and immobilized UDP

In view of the above results, PEI and PAA-activated agarose supports were selected to co-immobilize the UDP together with UGT and SuSyAc enzymes. This type of cationic polymeric supports promotes the strong adsorption of enzymes by anion exchange [51]. The resulting self-sufficient heterogeneous biocatalysts, in which the cofactor and the

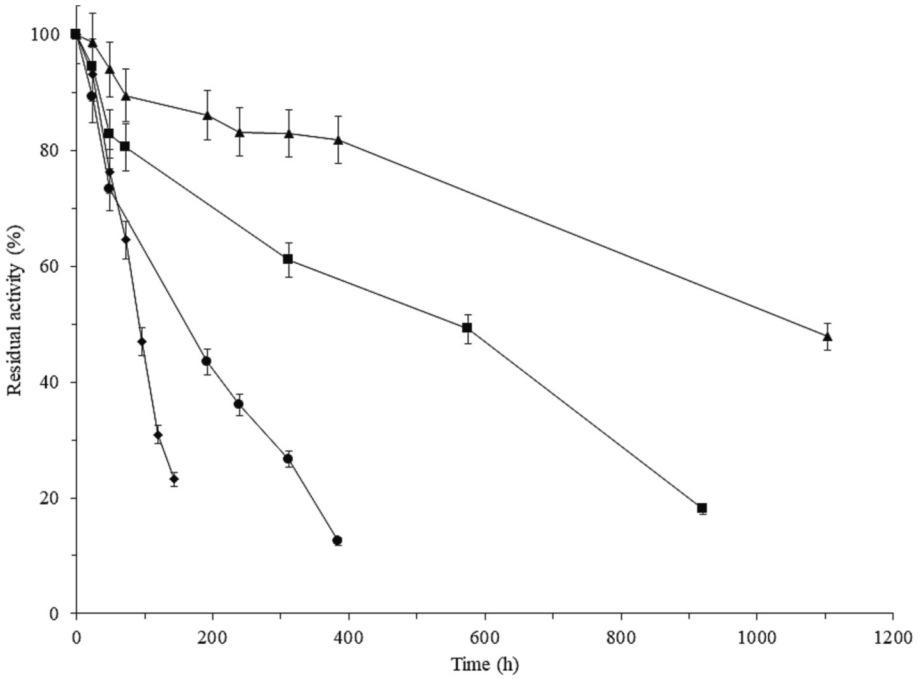

Fig. 2. Stability of different immobilized UDP preparations at optimal reaction conditions: 30 °C and pH 7.0. Symbols: (◆) free UDP, (■) UDP immobilized on PEI-Ag (▲) UDP immobilized on PAA-Ag and (●) UDP immobilized on DEAE-Sepharose.

two enzymes were co-immobilized, were functionally characterized in the glycosylation of piceid (resveratrol 3-β-D-glucoside).

Initially, we developed the co-immobilized biocatalyst of UGT and SuSyAc on PEI-Ag (SuSyAc-UGT-PEI-Ag biocatalyst). The immobilization conditions used were the optimal ones previously reported [21] and detailed in the methods section. Under these immobilization conditions, the two enzymes were spatially uniformly distributed throughout the porous agarose microstructure. This fact led to an increase in the efficiency of cofactor recycling. The immobilization parameters of SuSyAc and UGT on PEI-Ag are shown in Table 1. Both immobilization yield and the expressed activity ranged between 85 and 95%. These results are similar to those previously obtained for SuSyAc wild-type immobilization on PEI-Ag [21].

Next, we used the resulting heterogeneous biocatalysts to perform the piceid glycosylation reaction by either adding 50 μM of exogenous UDP (Fig. S2A) or 50 μM of co-immobilized UDP on the same support (0.33 $\mu mol_{UDP} \times g^{-1}$ of support) (Fig. S2B). The initial glycosylation reaction rates and other reaction parameters were compared (Table 2). Both glycosylation reactions exhibited a similar conversion and reaction rate without significant differences, reaching 100% of piceid glycosylation in 16 h. These results indicate that adsorption of the phosphorylated cofactor to the cationic support does not change the efficiency or initial rates of glycosylation, because UDP is in an associated/dissociated equilibrium with the positively-charged polymer-activated support that makes it available for the SuSyAc enzyme that converts sucrose and UDP into UDP-glucose.

Furthermore, UGT and SuSyAc were also co-immobilized on PAA-Ag (SuSyAc-UGT-PAA-Ag biocatalyst). The immobilization parameters of this new biocatalyst are shown in Table 1 and immobilization time-courses in Fig. S3. The immobilization yields were around 79% for UGT and 87% for SuSyAc. The expressed activity values were 81% for UGT and 87% for SuSyAc. To evaluate the functionality of this biocatalyst, the glycosylation reaction of 500 μM of piceid was conducted with the same amount of immobilized UDP as used above (50 μM of UDP, 0.33 $\mu mol_{UDP} \times g^{-1}$ of support). The SuSyAc-UGT-PAA-Ag biocatalyst catalyzed the glycosylation reaction (Fig. S2C) with the same efficiency as the SuSyAc-UGT-PEI-Ag biocatalyst (Fig. S2A and Fig. S2B) achieving 100% of glycosylation after 16 h. At this point, we hypothesized that the higher stability of UDP when immobilized on this support could contribute to a higher reusability of the SuSyAc-UGT-PAA-Ag and SuSyAc-UGT-PEI-Ag biocatalysts.

To prove this hypothesis, four batch reaction cycles were performed to evaluate the reusability of both self-sufficient biocatalysts, each containing 50 μM of co-immobilized UDP (Fig. 3). These self-sufficient biocatalysts were compared with the SuSyAc-UGT-PEI-Ag biocatalyst and UDP cofactor in soluble form (where fresh cofactor needs to be added at the start of each reaction cycle). The glycosylation reaction performed with the self-sufficient SuSyAc-UGT-PEI-Ag biocatalyst showed an accumulated TTN of 40 during four consecutive batch reaction cycles (the theoretical maximum) (Fig. 3 and Table 2). While, when the same self-sufficient biocatalyst was used but with soluble UDP, 100% of piceid conversion was also achieved during four consecutive batch reaction cycles. Although in this case, the accumulated TTN was only 10 because fresh cofactor had to be added at the beginning of each reaction cycle. It should be noted that, as previously described, piceid glycosylation with soluble SuSyAc and UGT enzymes yielded a TTN of 5 and without *in situ* UDP-glucose production 0.4 [41]. Enzyme and cofactor leaching was not detected in the wash steps between each reaction cycle (Table S2 and Fig. S4).

Table 1
Co-immobilization of SuSyAc and UGT on different cationic supports.

Biocatalyst	SuSyAc		UGT	
	Immobilization yield (%)[a]	Expressed activity (%)[a,b]	Immobilization yield (%)[a]	Expressed activity (%)[a]
SuSyAc-UGT-PEI-Ag	90 ± 5	87 ± 4	86 ± 3	95 ± 4
SuSyAc-UGT-PAA-Ag	87 ± 4	87 ± 3	79 ± 2	81 ± 3
$SuSyAc_{mut}$-UGT-PEI-Ag	90 ± 6	87 ± 3	89 ± 3	93 ± 5

[a] Immobilization yield and expressed activity were calculated as described in Methods section.
[b] Expressed activity after reduction step under optimal conditions.

The glycosylation reaction of piceid was also performed with the self-sufficient heterogeneous biocatalyst based on PAA-Ag support. In this case, an accumulated TTN of 35.2 was reached during four consecutive batch reaction cycles (Fig. 3 and Table 2). This result suggests that a higher amount of primary amino groups can contribute to higher cofactor stability, but this does not correlate with better biocatalyst reusability. Thus, although UDP adsorbed on the PAA-Ag support displays better stability (Fig. 2), its lower K_d^{app} could explain the results observed for the piceid glycosylation catalyzed by the SuSyAc-UGT-PAA-Ag biocatalyst. Here, the UDP is more strongly adsorbed to the support than in the case of PEI-Ag as it was also demonstrated by the ionic strength required to desorb the cofactor from these supports (Fig. 1). Consequently, the UDP in the self-sufficient SuSyAc-UGT-PAA-Ag biocatalyst would be less available for the enzymes and this is supported by a lower turnover frequency (TOF) (Table 2), which determines the efficiency with which the cofactor is regenerated [52]. As a result, the self-sufficient SuSyAc-UGT-PEI-Ag biocatalyst exhibited the highest TOF, a similar performance to those offered by the same biocatalyst with exogenously added cofactor, and it was therefore selected as the preferred catalyst for further optimization.

In the optimal configuration proposed here, PEI was irreversibly bound to the agarose microbeads, while the enzymes were bound to the PEI-coated support by relatively strong ionic adsorption. In addition, we incorporated the UDP cofactor to the solid phase, which was ionically adsorbed onto the cationic polymer. Thus, this adsorption was dynamic, allowing some cofactors to bind to the polymer and be reused in aqueous media, while others are dissociated but are trapped in the pore and available for enzymes [33]. Therefore, the catalytically active enzymes were surrounded by the cofactor, which was catalytically available but also retained in the solid phase for reuse over several reaction cycles.

The increased glycosylation rate could be due to the proximity effects of UGT and SuSy co-immobilization/co-localization on the porous surface of the solid support. Our results demonstrated that co-immobilization of UGT and SuSy was 3.2-fold more beneficial than immobilization of individual enzymes on separate carrier particles in the glycosylation of piceid from sucrose-derived UDP-glucose (Table 2). This effect was probably due to a higher efficiency of the UDP-glucose recycling (increased TOF) that can probably be attributed to the shortened diffusion distances of co-localized enzymes on the same porous surface of the solid support. These results are in agreement with the benefits obtained by the co-immobilization of glycosyltransferases and sucrose synthases described by Nidetzky and co-workers and our group [2,21].

3.5. Optimization of the glycosylation reactions

3.5.1. The importance of the composition of the medium reaction in glycosylation reactions

An important parameter to take into account in glycosylation reactions is the composition of the reaction medium and its pH. Lepak et al. established pH between 7.0 and 9.0 as the optimal pH range to perform piceid glycosylation [41]. Furthermore, as shown above, maintaining the UDP association/dissociation equilibirum with the cationic support is a key factor for the success of the process.

Table 2
Parameters of the glycosylation reactions of piceid with different co-immobilized biocatalysts.

Biocatalyst	UDP	UDP (μM)	V_0 (μM/h)	Yield (%)	TOF (h^{-1})[a]	TTN (mol product mol UDP^{-1})	Ref.
SuSyAc-PEI-Ag + UGT-PEI-Ag[f]	Soluble	100	30.9	65	0.309	3.25	[21]
SuSyAc-UGT-PEI-Ag	Soluble	50	48.8 ± 2.4	100	0.976	10[b]	This work
SuSyAc-UGT-PEI-Ag	Immobilized	50	49.0 ± 2.4	100	0.98	40[c]	This work
SuSyAc-UGT-PAA-Ag	Immobilized	50	40.8 ± 1.7	100	0.816	30[d]	This work
$SuSyAc_{mut}$-UGT-PEI-Ag	Immobilized	50	55.0 ± 2.5	100	1.1	50[e]	This work

[a] TOF was calculated according to the equation V_0 /[cofactor]. Where V_0 is the initial velocity of the main reaction and [cofactor] referred to the concentration of the cofactor in the reaction batch.
[b] Yield and TTN after one reaction cycle.
[c] TTN after 4 batch reaction cycles.
[d] TTN after 3 batch reaction cycles.
[e] TTN after 5 batch reaction cycles.
[f] Enzymes immobilized separately on PEI-Ag.

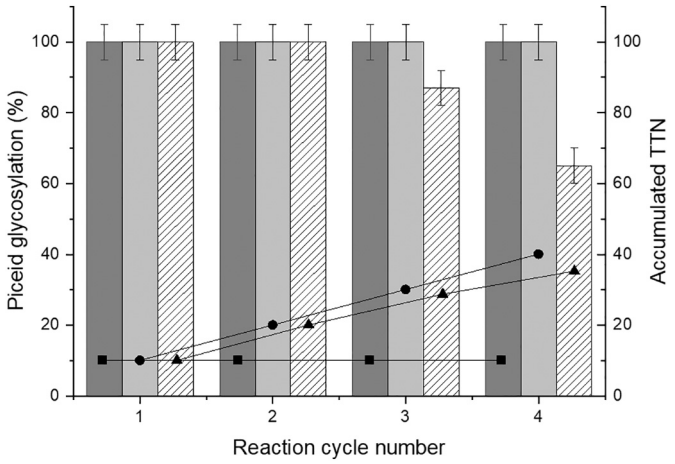

Fig. 3. Glycosylation reaction of piceid catalyzed by different co-immobilized biocatalysts. Symbols: Glycosilation reaction catalyzed by SuSyAc-UGT-PEI-Ag biocatalyst with soluble UDP (dark grey bars) and TTN (black squares); glycosylation reaction catalyzed by SuSyAc-UGT-PEI-Ag biocatalyst with UDP co-immobilized on the same support (light grey bars) and TTN (black circles); and glycosylation reaction catalyzed by SuSyAc-UGT-PAA-Ag biocatalyst (striped white bars) with co-immobilized UDP on the same support and TTN (black triangles). Reactions were performed with 0.25 g of biocatalyst in 1.7 mL of 50 mM HEPES at pH 7.0, 50 μM of UDP (soluble or immobilized), 100 mM sucrose, 500 μM of piceid and 10% of DMSO at 30 °C.

Thus, HEPES and Tris-HCl buffers were evaluated as reaction media. To perform this study, firstly, we performed the piceid glycosylation catalyzed by the co-immobilized SuSyAc-UGT-PEI-Ag biocatalyst using either 50 mM HEPES or Tris-HCl. As shown in Fig. S5A, the use of HEPES as reaction buffer increased the efficiency of piceid glycosylation 2-fold. This result is probably due to the fact that the sulphonic group of HEPES could compete with the phosphorylated cofactor for binding to the cationic carrier, favouring its release and availability to the enzyme molecules catalyzing the UDP-glucose regeneration reaction. In addition, we also evaluated the ideal concentration of HEPES to carry out the piceid glycosylation reaction (Fig. S5B). The concentration of HEPES at which the glycosylation reaction was conducted most efficiently was 50 mM, with an efficiency between 6 and 15% higher than the obtained at other studied concentrations (5, 25, 100 and 150 mM). In view of the above-mentioned results, HEPES was selected as the optimum buffer to perform glycosylation reactions and Tris-HCl buffer was preferred for cofactor immobilization.

3.5.2. Use of an improved variant of SuSyAc to boost glycosylation processes

In the context of the improvement of glycosylation processes, we aimed to compare the efficiency of glycosylation performed by a mutant of SuSyAc enzyme. Recently, Diricks et al. designed a variant of the SuSyAc enzyme ($SuSyAc_{mut}$) by rational mutagenesis that shows a reduced K_m for UDP (60-fold more affinity) and similar activities compared to the wild-type enzyme [34]. This variant consists of a double mutant in the QN motif of SuSyAc (L637M and T640V), introducing plant residues at positions in a putative nucleotide-binding motif surrounding the nucleobase ring of nucleoside diphosphate (NDP). Therefore, the use of an enhanced variant of SuSyAc with an improved K_m for UDP could be an advantage in the glycosylation reactions since it can lead to a reduction in the use of this cofactor, and a decrease in the overall process costs.

In this way, the improved SuSyAc variant was co-immobilized together with the UGT on PEI-Ag support. As shown in Table 1, the immobilization parameters were very similar to those previously obtained for the co-immobilization of the SuSyAc wild-type and UGT on the same support. The kinetic parameters of the two SuSyAc variants were determined in both soluble and immobilized forms (Table 3) using the bicinchoninic acid (BCA) assay [34]. K_m values for UDP ranged from 0.8 to 1.3 mM, which is comparable to the values reported for plant enzymes [15,18,34]. No significant differences were found between in the affinity for UDP in both the soluble and immobilized forms of SuSyAc and $SuSyAc_{mut}$. $SuSyAc_{mut}$ showed a lower K_m for UDP and a higher associated maximal velocity (V_{max}) than the SuSyAc wild-type, which could result in enhanced coupled reactions due to the higher affinity of the SuSyAc variant for UDP.

3.5.3. Piceid glycosylation using the self-sufficient $SuSyAc_{mut}$-UGT-PEI-Ag biocatalyst

With the aim of achieving more efficient glycosylation reactions, five consecutive batch piceid glycosylation reactions were carried out comparing both SuSyAc variants. For this purpose, 50 μM of immobilized UDP (0.33 μmol UDP × g^{-1} support) was co-immobilized together with UGT and SuSyAc enzymes. The self-sufficient $SuSyAc_{mut}$-UGT-PEI-Ag biocatalyst was able to reach an accumulated TTN value of 50 (theoretical maximum) after five consecutive batch reaction cycles without the need to add exogenous cofactor (Fig. 4 and Table 2). While,

Table 3
Kinetic parameters of the enzymes SuSyAc wild type and $SuSyAc_{mut}$ in their soluble and co-immobilized forms.

	Soluble SuSyAc	Immobilized SuSyAc	Soluble $SuSyAc_{mut}$	Immobilized $SuSyAc_{mut}$
V_{max} (U/mL)	14.38 ± 0.71	12.16 ± 0.60	26.92 ± 1.30	17.45 ± 0.91
V_{max} (U/mg)	20.87 ± 1.10	13.66 ± 0.70	46.42 ± 2.32	32.19 ± 1.64
K_m (mM)	1.16 ± 0.06	1.27 ± 0.07	0.83 ± 0.04	0.87 ± 0.05

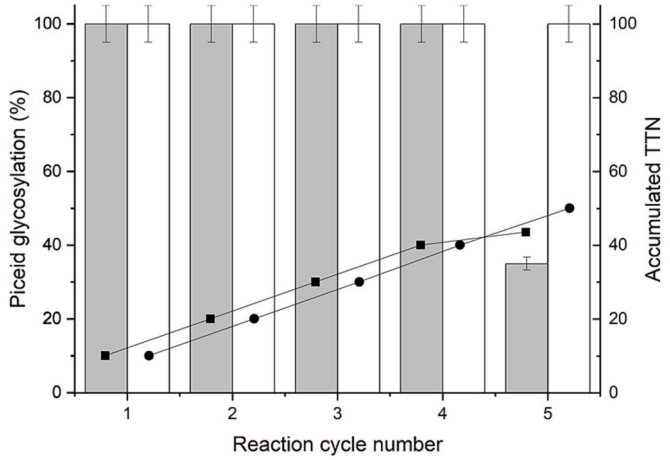

Fig. 4. Glycosylation reaction of piceid catalyzed by self-sufficient biocatalysts. Symbols: reaction catalyzed by SuSyAc-UGT-PEI-Ag biocatalyst with co-immobilized UDP (grey bars) and TTN (black squares); and reaction catalyzed by SuSyAc$_{mut}$-UGT-PEI-Ag biocatalyst with UDP co-immobilized (white bars) and TTN (black circles). Reaction medium was composed of 0.25 g of biocatalyst in 1.7 mL of 50 mM HEPES at pH 7.0, 50 μM of UDP (soluble or immobilized), 100 mM sucrose, 500 μM of piceid and 10% of DMSO at 30 °C.

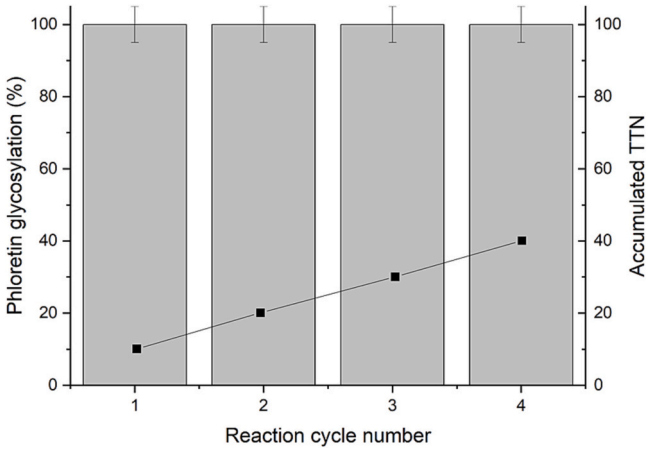

Fig. 5. Glycosylation of quercetin catalyzed by SuSyAc$_{mut}$-UGT-Ag-PEI25 biocatalyst with UDP co-immobilized. Reaction medium was composed of 0.25 g of biocatalyst in 1.7 mL of 50 mM HEPES pH 8.0, 50 μM of UDP (soluble or immobilized), 100 mM sucrose, 500 μM of quercetin and 25% of DMSO at 30 °C. Symbols: grey bars show the efficiency of glycosylation and squares indicate the accumulated TTN.

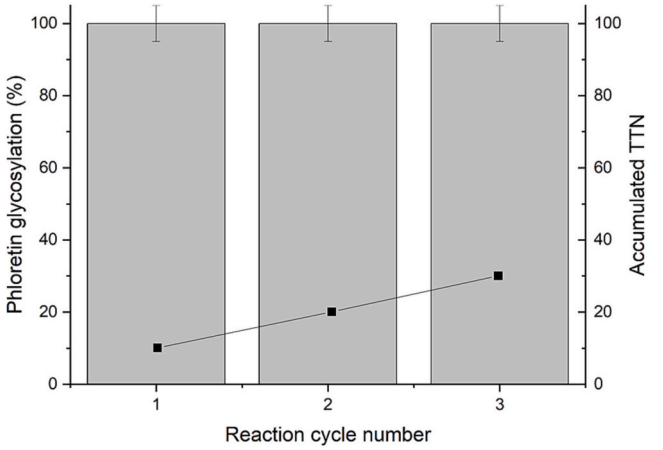

Fig. 6. Glycosylation of phloretin catalyzed by SuSyAc$_{mut}$-UGT-Ag-PEI25 biocatalyst with UDP co-immobilized. Reaction medium was composed of 0.25 g of biocatalyst in 1.7 mL of 50 mM HEPES pH 7.0, 50 μM of UDP (soluble or immobilized), 100 mM sucrose, 500 μM of phloretin and 25% of DMSO at 30 °C. Symbols: grey bars indicate the efficiency of glycosylation and squares show the accumulated TTN.

the self-sufficient SuSyAc-UGT-PEI-Ag biocatalyst reached a TTN of 43.5 without adding exogenous UDP. This result was accompanied by a decrease in the rate of the glycosylation reaction from the fifth reaction cycle which is probably due to a decreased availability of cofactor (data not shown). In the case of the self-sufficient SuSyAc$_{mut}$-UGT-PEI-Ag biocatalyst, the observed increases in the reaction parameters such as TTN, V_0 and TOF (Table 2) could be explained by the higher affinity of SuSyAc$_{mut}$ for UDP, which allowed achieving 100% of glycosylation in five consecutive batch reaction cycles without adding soluble UDP. Thus, the lower K_m of SuSyAc$_{mut}$ seems to favour the overall reaction, since it requires a lower effective concentration of UDP to perform glycosylation reactions as efficiently as the wild type.

3.6. Glycosylation of quercetin and phloretin catalyzed by the self-sufficient SuSyAc$_{mut}$-UGT-PEI-Ag biocatalyst

Finally, as UGT is capable of glycosylate up to 12 different flavonoid compounds [53,54], we expanded the versatility of the optimal self-sufficient biocatalyst in the glycosylation of other polyphenolic compounds such as quercetin and phloretin.

On the one hand, the self-sufficient SuSyAc$_{mut}$-UGT-PEI-Ag biocataly reached 100% of conversion during four consecutive batch reaction cycles, glycosylating a total of 2000 μM of quercetin using only 50 μM of immobilized UDP (Fig. 5). The accumulated TTN during four batch consecutive cycles under operational conditions was 40. This result represents a significant improvement (around 460-fold more efficient) compared to previous studies on glycosylation of this compound [35,55].

On the other hand, the glycosylation of phloretin catalyzed by the optimal self-sufficient biocatalyst yielded almost 100% in 3 consecutive batch reaction cycles (Fig. 6), reaching an accumulated TTN value of 30, which represents an increase of 3-fold compared to literature [1].

3.7. Identification of glycosylated compounds by RP-HPLC–ESI-Q-TOF-MS

RP-HPLC–ESI-Q-TOF-MS is a powerful analytical tool for characterizing and quantifying individual phenolic compounds [56–58]. Samples of glycosylation reactions catalyzed by the optimal self-sufficient heterogeneous biocatalyst were analyzed using HPLC-ESI-QTOF Maxis II with negative electrospray technique for the determination of its exact mass (Tables S3-S5) [59]. Figs. S6, S7 and S8 show the combined base peak chromatograms of HPLC-UV and MS obtained from the glycosylation reactions at 6 h reaction time of piceid, quercetin and phloretin, respectively.

In the combined base peak chromatogram of piceid glycosylation reaction catalyzed by the self-sufficient SuSyAc$_{mut}$-UGT-PEI-Ag biocatalyst (Fig. S6), two major peaks appear, compound 1 (C1) and compound 3 (C3). C1 with $[M-H]^-$ *m/z* at 597.18 (dominant precursor ion with R_t 7.5 min), exhibiting characteristic fragment ions at *m/z* 227 $[C_{14}H_{11}O_3]^-$ and *m/z* 389 $[C_{20}H_{21}O_8]^-$, was identified as resveratrol-3,5-diglucoside ($C_{27}H_{33}O_{15}$), which represents the adduct composed of resveratrol-3,5-diglucoside ($C_{26}H_{31}O_{13}$) and formic acid (CH_2O_2) (Table S3). The second major peak C3 (R_T 9.2 min) was also characterized and compared to standard trans-piceid. C3 with a $[M-H]^-$ *m/z* at 435.13 exhibited characteristic ions fragments at *m/z* 389.12 $[C_{20}H_{21}O_8]^-$ and 227.1 $[C_{14}H_{11}O_3]^-$, which corresponds to resveratrol 3-*O*-beta-D-glucoside and resveratrol. C3 was identified as the adduct consisting of the piceid and formic acid $[C_{21}H_{23}O_{10}]^-$. For further

details, the reader is referred to the following reference [21]. Notably, glycosylated resveratrol derivatives could be promising agents for the development of new treatments against neurodegenerative diseases as they have been shown to be neuroprotective in some experimental models [60]. In particular, resveratrol 3,5-β-D-diglucoside have also shown to be a potential prodrug for the treatment of inflammatory bowel disease [61]. Furthermore, it has been demonstrated that 3,5-diglucoside is more water-soluble and resistant to enzymatic hydrolysis than piceid and resveratrol, while still maintaining most of its antioxidant capacity [41].

In the case of the glycosylation reaction of quercetin, isotopic patterns of ions of main peaks were evaluated (Fig. S7). The chromatogram at 280 nm and ESI-Q-TOF-MS detection showed a main peak with a higher intensity at R_t 9.0 min, which corresponded to compound 21 (C21). C21 was characterized by both MS/MS fragmentation patterns and retention time as compared with the authentic standard. The identity of the C21 was confirmed as quercetin-3-*O*-glucoside by the detection of an $[M–H]^-$ ion at *m/z* 463.08, having the formula $[C_{21}H_{19}O_{12}]^-$. The loss of glucose (162 Da) resulting in a product ion at *m/z* 301.03 visible in the MS/MS spectrum. Reference standard for quercetin-3-*O*-glucoside also corresponded to C21. While, compounds C16 (C16, R_t 8.0 min) and 17 (C17, Rt 8.2 min) were a pair of isomers with an $[M–H]^-$ ion at *m/z* 625.14, which corresponded to diglucosylated quercetin with the same dominant precursor ion at *m/z* 625.14 with the same proposed formula $[C_{27}H_{29}O_{17}]^-$. The MS/MS spectra of these two compounds were identical, producing the 463.08 ion $[C_{21}H_{19}O_{12}]^-$, which was derived from the loss of one glucose molecule. The last peak of this chromatogram profile, compound 28 (C28) (R_t 11.9 min) represent the ion precursor with a *m/z* 301.03 $[C_{15}H_9O_7]^-$, this was consistent with the compound quercetin, the substrate of the reaction (Table S4). Reference standard for quercetin also corresponded to C28. Quercetin-3-*O*-glucoside and quercetin have shown similar antioxidant [62], antifungal, antiviral, antidiabetic, antiobesity [63] capacity and neuroprotective effects with improved water solubility, bioavailability [62,64]. Whereas, quercetin-3-*O*-glucoside has demonstrated a more potent antiproliferative effect than quercetin on various cancer cell lines [62].

The combined base peak chromatogram of phloretin glycosylation reaction is shown in Fig. S8. Compound 14 (C14) had a R_t of 10.2 min with a $[M - H]^-$ ion at 435.13, which corresponded to exactly the same mass as monoglucoside of phloretin $[C_{21}H_{23}O_{10}]$ (Table S5). The identity of C14 was confirmed with a pure standard of phloridzin (phloretin 2′-*O*-glucoside). Other less intense ions were detected at *m/z* 471.10 $[M - H + HCl]^-$, 481.13 $[M - H + HCO_2H]^-$ and 549.12 $[M - H + HCO_2H + HCO_2Na]^-$. Compound 15 (C15, R_t 10.6 min) displayed identical $[M - H]^-$ ion at *m/z* at 435.13 $[C_{21}H_{23}O_{10}]$, which could correspond to phloretin 4-*O*-glucoside. The formation of secondary glycosylated compounds when the glycosylation reaction is coupled with UDP-glucose regeneration systems has been previously observed by Terasaka et al. [20], particularly in enzymes that are sensitive to UDP inhibition. The presence of phloretin ($[M - H]^-$ ion at *m/z* at 273.077, having the formula $[C_{15}H_3O_5]$) was also confirmed by comparison of R_t (12.8 min) of pure standard. Phloridzin can be compared to phloretin in terms of bioactive properties such as antioxidant, antifungal [65], anti-inflammatory [66], anti-diabetic activities [67,68] and anti-cancer [69]. However, it has lower toxicity and higher bioavailability [70,71].

4. Conclusions

The development of self-sufficient heterogeneous biocatalysts allows for the joint reuse of both the enzyme and the cofactor, increasing their lifespan and the profitability of cofactor-dependent processes [27,72,73]. Herein, we have expanded the fabrication of self-sufficient heterogeneous biocatalysts for the glycosylation of polyphenolic compounds. For this purpose, we have developed a multi-functional and self-sufficient immobilized system composed of a robust variant of sucrose synthase ($SuSyAc_{mut}$) with a lower k_m value for UDP, a versatile glycosyltransferase (UGT) that perform the main reaction of glycosylation of polyphenolic compounds, and the negative-charged phosphorylated UDP cofactor. All the biological elements were incorporated into the solid phase, in this case a polycationic-modified support that facilitated the adsorption of the negatively charged cofactor. The results obtained in this work indicated that the self-sufficient $SuSyAc_{mut}$-UGT-PEI-Ag biocatalyst was able to catalyze glycosylation reactions of different bioactive compounds (piceid, quercetin and phloretin) with *in situ* regeneration of the UDP-glucose, allowing multiple consecutive reaction cycles without the addition of exogenous cofactor. Therefore, the development of self-sufficient heterogeneous biocatalytic systems offers the opportunity to develop more cost-effective glycosylation processes contributing to make biocatalysis more efficient and sustainable. However, more effort should be focused on the development of improved self-sufficient heterogeneous biocatalysts which, through the use of advanced immobilization materials and improved enzymes, would allow such biocatalysts to be used for longer continuous flow operation times or a higher number of consecutive reaction cycles.

CRediT authorship contribution statement

Lara Trobo-Maseda: Methodology, Investigation, Formal analysis, Writing- Original draft preparation. **Maria Romero-Fernandez:** Methodology, Validation, Data curation. **José M. Guisan**: Conceptualization, Supervision, Writing- Reviewing and Editing, Funding acquisition. **Javier Rocha-Martin**: Conceptualization, Supervision, Visualization Writing- Original draft preparation, Writing- Reviewing and Editing.

Declaration of competing interest

Jose M. Guisan reports financial support was provided by European Commission Seventh Framework Programme for Research and Technological Development Euratom.

Data availability

Data will be made available on request.

Acknowledgments

This work was supported by the EU FP7 project SuSy (Sucrose Synthase as Cost-Effective Mediator of Glycosylation Reactions, C-KBBE/3293). Prof. Tom Desmet and Dr. Margo Diricks (Centre for Industrial Biotechnology and Biocatalysis, Ghent University, Belgium) kindly provided the plasmid for expression of the different SuSyAc variants. Prof. Bernd Nidetzky and Dr. Alexander Gutmann (Institute of Biotechnology and Biochemical Engineering, Graz University, Austria) are gratefully acknowledged for their kind help and for providing the plasmid for the expression of UGT71A15. The enzyme production was carried out in the 'CBMSO Fermentation Facility'. We thank the Mass Spectrometry Laboratory (Interdepartmental Investigation Service (SIdI), Autonomous University of Madrid) for providing facilities and technical assistance for RP-HPLC–ESI-Q-TOF-MS analysis, in particular to Dr. Maria Teresa Alonso Pascual.

Appendix A. Supplementary data

Supplementary data to this article can be found online at https://doi.org/10.1016/j.ijbiomac.2023.126009.

References

[1] L. Bungaruang, A. Gutmann, B. Nidetzky, Leloir glycosyltransferases and natural product glycosylation: biocatalytic synthesis of the C-glucoside nothofagin, a major antioxidant of redbush herbal tea, Adv. Synth. Catal. 355 (14–15) (2013) 2757–2763, https://doi.org/10.1002/adsc.201300251.

[2] H. Liu, G. Tegl, B. Nidetzky, Glycosyltransferase co-immobilization for natural product glycosylation: Cascade biosynthesis of the c-glucoside nothofagin with efficient reuse of enzymes, Adv. Synth. Catal. 363 (8) (2021) 2157–2169, https://doi.org/10.1002/adsc.202001549.
[3] J. Ati, P. Lafite, R. Daniellou, Enzymatic synthesis of glycosides: from natural *O*- and *N*-glycosides to rare *C*- and *S*-glycosides, Beilstein J. Org. Chem. 13 (2017) 1857–1865, https://doi.org/10.3762/bjoc.13.180.
[4] K. Olsson, S. Carlsen, A. Semmler, E. Simón, M.D. Mikkelsen, B.L. Møller, Microbial production of next-generation stevia sweeteners, Microb. Cell Factories 15 (1) (2016) 207, https://doi.org/10.1186/s12934-016-0609-1.
[5] L. Sánchez-del-Campo, M. Sáez-Ayala, S. Chazarra, J. Cabezas-Herrera, J. N. Rodríguez-López, Binding of natural and synthetic polyphenols to human dihydrofolate reductase, Int. J. Mol. Sci. 10 (12) (2009) 5398–5410, https://doi.org/10.3390/ijms10125398.
[6] C. Saint-Jore-Dupas, L. Faye, V. Gomord, From planta to pharma with glycosylation in the toolbox, Trends Biotechnol. 25 (7) (2007) 317–323, https://doi.org/10.1016/j.tibtech.2007.04.008.
[7] G. Walsh, Post-translational modifications of protein biopharmaceuticals, Drug Discov. Today 15 (17) (2010) 773–780, https://doi.org/10.1016/j.drudis.2010.06.009.
[8] I. Antonopoulou, S. Varriale, E. Topakas, U. Rova, P. Christakopoulos, V. Faraco, Enzymatic synthesis of bioactive compounds with high potential for cosmeceutical application, Appl. Microbiol. Biotechnol. 100 (15) (2016) 6519–6543, https://doi.org/10.1007/s00253-016-7647-9.
[9] F. De Bruyn, J. Maertens, J. Beauprez, W. Soetaert, M. De Mey, Biotechnological advances in UDP-sugar based glycosylation of small molecules, Biotechnol. Adv. 33 (2) (2015) 288–302, https://doi.org/10.1016/j.biotechadv.2015.02.005.
[10] W. Schwab, T.C. Fischer, A. Giri, M. Wüst, Potential applications of glucosyltransferases in terpene glucoside production: impacts on the use of aroma and fragrance, Appl. Microbiol. Biotechnol. 99 (1) (2015) 165–174, https://doi.org/10.1007/s00253-014-6229-y.
[11] R.P. Pandey, P. Bashyal, P. Parajuli, T. Yamaguchi, J.K. Sohng, Two trifunctional Leloir glycosyltransferases as biocatalysts for natural products glycodiversification, Org. Lett. 21 (19) (2019) 8058–8064, https://doi.org/10.1021/acs.orglett.9b03040.
[12] N. Putkaradze, D. Teze, F. Fredslund, D.H. Welner, Natural product *C*-glycosyltransferases – a scarcely characterised enzymatic activity with biotechnological potential, Nat. Prod. Rep. 38 (3) (2021) 432–443, https://doi.org/10.1039/D0NP00040J.
[13] T. Desmet, W. Soetaert, P. Bojarová, V. Křen, L. Dijkhuizen, V. Eastwick-Field, A. Schiller, Enzymatic glycosylation of small molecules: challenging substrates require tailored catalysts, Chem. Eur. J. 18 (35) (2012) 10786–10801, https://doi.org/10.1002/chem.201103069.
[14] B. Nidetzky, A. Gutmann, C. Zhong, Leloir glycosyltransferases as biocatalysts for chemical production, ACS Catal. 8 (7) (2018) 6283–6300, https://doi.org/10.1021/acscatal.8b00710.
[15] A. Gutmann, A. Lepak, M. Diricks, T. Desmet, B. Nidetzky, Glycosyltransferase cascades for natural product glycosylation: use of plant instead of bacterial sucrose synthases improves the UDP-glucose recycling from sucrose and UDP, Biotechnol. J. 12 (7) (2017) 1600557, https://doi.org/10.1002/biot.201600557.
[16] J. Pei, A. Chen, Q. Sun, L. Zhao, F. Cao, F. Tang, Construction of a novel UDP-rhamnose regeneration system by a two-enzyme reaction system and application in glycosylation of flavonoid, Biochem. Eng. J. 139 (2018) 33–42, https://doi.org/10.1016/j.bej.2018.08.007.
[17] Y. Zhang, S. Xu, Y. Jin, Y. Dai, Y. Chen, X. Wu, Efficient biocatalytic preparation of rebaudioside KA: highly selective glycosylation coupled with UDPG regeneration, Sci. Rep. 10 (1) (2020) 6230, https://doi.org/10.1038/s41598-020-63379-9.
[18] K. Schmölzer, A. Gutmann, M. Diricks, T. Desmet, B. Nidetzky, Sucrose synthase: a unique glycosyltransferase for biocatalytic glycosylation process development, Biotechnol. Adv. 34 (2) (2016) 88–111, https://doi.org/10.1016/j.biotechadv.2015.11.003.
[19] K. Schmölzer, M. Lemmerer, A. Gutmann, B. Nidetzky, Integrated process design for biocatalytic synthesis by a Leloir glycosyltransferase: UDP-glucose production with sucrose synthase, Biotechnol. Bioeng. 114 (4) (2017) 924–928, https://doi.org/10.1002/bit.26204.
[20] K. Terasaka, Y. Mizutani, A. Nagatsu, H. Mizukami, In situ UDP-glucose regeneration unravels diverse functions of plant secondary product glycosyltransferases, FEBS Lett. 586 (24) (2012) 4344–4350, https://doi.org/10.1016/j.febslet.2012.10.045.
[21] L. Trobo-Maseda, A.H. Orrego, J.M. Guisan, J. Rocha-Martin, Coimmobilization and colocalization of a glycosyltransferase and a sucrose synthase greatly improves the recycling of UDP-glucose: glycosylation of resveratrol 3-O-β-D-glucoside, Int. J. Biol. Macromol. 157 (2020) 510–521, https://doi.org/10.1016/j.ijbiomac.2020.04.120.
[22] L.-J. Zhang, D.-G. Wang, P. Zhang, C. Wu, Y.-Z. Li, Promiscuity characteristics of versatile plant glycosyltransferases for natural product glycodiversification, ACS Synth. Biol. 11 (2) (2022) 812–819, https://doi.org/10.1021/acssynbio.1c00489.
[23] D.-M. Liang, J.-H. Liu, H. Wu, B.-B. Wang, H.-J. Zhu, J.-J. Qiao, Glycosyltransferases: mechanisms and applications in natural product development, Chem. Soc. Rev. 44 (22) (2015) 8350–8374, https://doi.org/10.1039/C5CS00600G.
[24] L. Mestrom, M. Przypis, D. Kowalczykiewicz, A. Pollender, A. Kumpf, S.R. Marsden, I. Bento, A.B. Jarzębski, K. Szymańska, A. Chruściel, D. Tischler, R. Schoevaart, U. Hanefeld, P.-L. Hagedoorn, Leloir glycosyltransferases in applied biocatalysis: a multidisciplinary approach, Int. J. Mol. Sci. 20 (21) (2019) 5263, https://doi.org/10.3390/ijms20215263.
[25] S. Velasco-Lozano, F. López-Gallego, Wiring step-wise reactions with immobilized multi-enzyme systems, Biocatalysis and Biotransformation 36 (3) (2018) 184–194, https://doi.org/10.1080/10242422.2017.1310208.
[26] R.A. Sheldon, A. Basso, D. Brady, New frontiers in enzyme immobilisation: robust biocatalysts for a circular bio-based economy, Chem. Soc. Rev. 50 (10) (2021) 5850–5862, https://doi.org/10.1039/D1CS00015B.
[27] J. Rocha-Martín, B. de la Rivas, R. Muñoz, J.M. Guisán, F. López-Gallego, Rational co-immobilization of bi-enzyme cascades on porous supports and their applications in bio-redox reactions with insitu recycling of soluble cofactors, ChemCatChem 4 (9) (2012) 1279–1288, https://doi.org/10.1002/cctc.201200146.
[28] C. Schmid-Dannert, F. López-Gallego, Advances and opportunities for the design of self-sufficient and spatially organized cell-free biocatalytic systems, Curr. Opin. Chem. Biol. 49 (2019) 97–104, https://doi.org/10.1016/j.cbpa.2018.11.021.
[29] J.M. Bolivar, A. Hidalgo, L. Sánchez-Ruiloba, J. Berenguer, J.M. Guisán, F. López-Gallego, Modulation of the distribution of small proteins within porous matrixes by smart-control of the immobilization rate, J. Biotechnol. 155 (4) (2011) 412–420, https://doi.org/10.1016/j.jbiotec.2011.07.039.
[30] A.H. Orrego, D. Andrés-Sanz, S. Velasco-Lozano, M. Sanchez-Costa, J. Berenguer, J. M. Guisan, J. Rocha-Martin, F. López-Gallego, Self-sufficient asymmetric reduction of β-ketoesters catalysed by a novel and robust thermophilic alcohol dehydrogenase co-immobilised with NADH, Catal. Sci. Technol. 11 (9) (2021) 3217–3230, https://doi.org/10.1039/D1CY00268F.
[31] A.I. Benítez-Mateos, E. San Sebastian, N. Ríos-Lombardía, F. Morís, J. González-Sabín, F. López-Gallego, Asymmetric reduction of prochiral ketones by using self-sufficient heterogeneous biocatalysts based on NADPH-dependent ketoreductases, Chem. Eur. J. 23 (66) (2017) 16843–16852, https://doi.org/10.1002/chem.201703475.
[32] X. Ji, Z. Su, P. Wang, G. Ma, S. Zhang, Tethering of nicotinamide adenine dinucleotide inside hollow nanofibers for high-yield synthesis of methanol from carbon dioxide catalyzed by coencapsulated multienzymes, ACS Nano 9 (4) (2015) 4600–4610, https://doi.org/10.1021/acsnano.5b01278.
[33] S. Velasco-Lozano, A.I. Benítez-Mateos, F. López-Gallego, Co-immobilized phosphorylated cofactors and enzymes as self-sufficient heterogeneous biocatalysts for chemical processes, Angew. Chem. Int. Ed. 56 (3) (2017) 771–775, https://doi.org/10.1002/anie.201609758.
[34] M. Diricks, A. Gutmann, S. Debacker, G. Dewitte, B. Nidetzky, T. Desmet, Sequence determinants of nucleotide binding in sucrose synthase: improving the affinity of a bacterial sucrose synthase for UDP by introducing plant residues, Protein Eng. Des. Sel. 30 (3) (2017) 143–150, https://doi.org/10.1093/protein/gzw048.
[35] E.K. Lim, D.A. Ashford, B. Hou, R.G. Jackson, D.J. Bowles, *Arabidopsis* glycosyltransferases as biocatalysts in fermentation for regioselective synthesis of diverse quercetin glucosides, Biotechnol. Bioeng. 87 (5) (2004) 623–631, https://doi.org/10.1002/bit.20154.
[36] C. Gosch, H. Flachowsky, H. Halbwirth, J. Thill, R. Mjka-Wittmann, D. Treutter, K. Richter, M.V. Hanke, K. Stich, Substrate specificity and contribution of the glycosyltransferase UGT71A15 to phloridzin biosynthesis, Trees - Structure and Function 26 (1) (2012) 259–271, https://doi.org/10.1007/s00468-011-0669-0.
[37] P.C.-T. Tang, Y.-F. Ng, S. Ho, M. Gyda, S.-W. Chan, Resveratrol and cardiovascular health – promising therapeutic or hopeless illusion? Pharmacol. Res. 90 (2014) 88–115, https://doi.org/10.1016/j.phrs.2014.08.001.
[38] Y. Takizawa, R. Nakata, K. Fukuhara, H. Yamashita, H. Kubodera, H. Inoue, The 4′-hydroxyl group of resveratrol is functionally important for direct activation of PPARα, PLoS One 10 (3) (2015), e0120865 https://doi.org/10.1371/journal.pone.0120865.
[39] D. Su, Y. Cheng, M. Liu, D. Liu, H. Cui, B. Zhang, S. Zhou, T. Yang, Q. Mei, Comparision of piceid and resveratrol in antioxidation and antiproliferation activities in vitro, PLoS One 8 (1) (2013), e54505, https://doi.org/10.1371/journal.pone.0054505.
[40] D. Treutter, Biosynthesis of phenolic compounds and its regulation in apple, Plant Growth Regul. 34 (1) (2001) 71–89, https://doi.org/10.1023/A:1013378702940.
[41] A. Lepak, A. Gutmann, S.T. Kulmer, B. Nidetzky, Creating a water-soluble resveratrol-based antioxidant by site-selective enzymatic glucosylation, ChemBioChem 16 (13) (2015) 1870–1874, https://doi.org/10.1002/cbic.201500284.
[42] D.B.F.M. Diricks, P. van Daele, M. Walmagh, T. Desmet, Identification of sucrose synthase in nonphotosynthetic bacteria and characterization of the recombinant enzymes, Appl. Microbiol. Biotechnol. 99 (20) (2015) 8465–8474, https://doi.org/10.1007/s00253-015-6548-7.
[43] L. Trobo-Maseda, A.H. Orrego, S. Moreno-Pérez, G. Fernández-Lorente, J. M. Guisan, J. Rocha-Martin, Stabilization of multimeric sucrose synthase from *Acidithiobacillus caldus* via immobilization and post-immobilization techniques for synthesis of UDP-glucose, Appl. Microbiol. Biotechnol. 102 (2) (2018) 773–787, https://doi.org/10.1007/s00253-017-8649-y.
[44] F. López-Gallego, G. Fernandez-Lorente, J. Rocha-Martín, J.M. Bolivar, C. Mateo, J. M. Guisan, Multi-point covalent immobilization of enzymes on glyoxyl agarose with minimal physico-chemical modification: Stabilization of industrial enzymes, in: J.M. Guisan, J.M. Bolivar, F. López-Gallego, J. Rocha-Martín (Eds.), Immobilization of Enzymes and Cells: Methods and Protocols, Springer, US, New York, NY, 2020, pp. 93–107.
[45] F.-L.R. Cesar Mateo, Guisan JM, reversible enzyme immobilization via a very strong and nondistorting ionic adsorption on support polyethyleneimine composites, Biotechnol. Bioeng. 68 (2000) 98–105, https://doi.org/10.1002/(SICI)1097-0290(20000405)68:1<98::AID-BIT12>3.0.CO;2-T.
[46] A.I. Benítez-Mateos, M.L. Contente, S. Velasco-Lozano, F. Paradisi, F. López-Gallego, Self-sufficient flow-biocatalysis by coimmobilization of pyridoxal 5′-

phosphate and ω-transaminases onto porous carriers, ACS Sustain. Chem. Eng. 6 (10) (2018) 13151–13159, https://doi.org/10.1021/acssuschemeng.8b02672.
[47] S. Kobayashi, K. Hiroishi, M. Tokunoh, T. Saegusa, Chelating properties of linear and branched poly(ethylenimines), Macromolecules 20 (7) (1987) 1496–1500, https://doi.org/10.1021/ma00173a009.
[48] J. Suh, H.J. Paik, B.K. Hwang, Ionization of poly(ethylenimine) and poly (allylamine) at various pH's, Bioorg. Chem. 22 (3) (1994) 318–327, https://doi.org/10.1006/bioo.1994.1025.
[49] B.-L. Johansson, M. Andersson, J. Lausmaa, P. Sjövall, Chemical characterisation of different separation media based on agarose by static time-of-flight secondary ion mass spectrometry, J. Chromatogr. A 1023 (1) (2004) 49–56, https://doi.org/10.1016/j.chroma.2003.10.008.
[50] A.Y. Kostritskii, D.A. Kondinskaia, A.M. Nesterenko, A.A. Gurtovenko, Adsorption of synthetic cationic polymers on model phospholipid membranes: insight from atomic-scale molecular dynamics simulations, Langmuir 32 (40) (2016) 10402–10414, https://doi.org/10.1021/acs.langmuir.6b02593.
[51] J.J. Virgen-Ortíz, J.C.S. dos Santos, Á. Berenguer-Murcia, O. Barbosa, R. C. Rodrigues, R. Fernandez-Lafuente, Polyethylenimine: a very useful ionic polymer in the design of immobilized enzyme biocatalysts, J. Mater. Chem. B 5 (36) (2017) 7461–7490, https://doi.org/10.1039/C7TB01639E.
[52] X. Wang, T. Saba, H.H.P. Yiu, R.F. Howe, J.A. Anderson, J. Shi, Cofactor NAD(P)H regeneration inspired by heterogeneous pathways, Chem 2 (5) (2017) 621–654, https://doi.org/10.1016/j.chempr.2017.04.009.
[53] C. Gosch, H. Flachowsky, H. Halbwirth, J. Thill, R. Mjka-Wittmann, D. Treutter, K. Richter, M.V. Hanke, K. Stich, Substrate specificity and contribution of the glycosyltransferase UGT71A15 to phloridzin biosynthesis, Trees 26 (1) (2012) 259–271, https://doi.org/10.1007/s00468-011-0669-0.
[54] C. Gosch, H. Halbwirth, B. Schneider, D. Hölscher, K. Stich, Cloning and heterologous expression of glycosyltransferases from *Malus* x *domestica* and *Pyrus communis*, which convert phloretin to phloretin 2′-*O*-glucoside (phloridzin), Plant Sci. 178 (3) (2010) 299–306, https://doi.org/10.1016/j.plantsci.2009.12.009.
[55] M.H. Son, B.G. Kim, D.H. Kim, M. Jin, K. Kim, J.H. Ahn, Production of flavonoid *O*-glucoside using sucrose synthase and flavonoid *O*-glucosyltransferase fusion protein, J. Microbiol. Biotechnol. 19 (7) (2009) 709–712, https://doi.org/10.4014/jmb.0811.608.
[56] Z. Zhu, B. Zhong, Z. Yang, W. Zhao, L. Shi, A. Aziz, A. Rauf, A.S.M. Aljohani, F. A. Alhumaydhi, H.A.R. Suleria, LC-ESI-QTOF-MS/MS characterization and estimation of the antioxidant potential of phenolic compounds from different parts of the Lotus (*Nelumbo nucifera*) seed and rhizome, ACS Omega 7 (17) (2022) 14630–14642, https://doi.org/10.1021/acsomega.1c07018.
[57] R. Moss, Q. Mao, D. Taylor, C. Saucier, Investigation of monomeric and oligomeric wine stilbenoids in red wines by ultra-high-performance liquid chromatography/electrospray ionization quadrupole time-of-flight mass spectrometry, Rapid Commun. Mass Spectrom. 27 (16) (2013) 1815–1827, https://doi.org/10.1002/rcm.6636.
[58] D. Kadam, S. Palamthodi, S.S. Lele, LC–ESI-Q-TOF–MS/MS profiling and antioxidant activity of phenolics from *L. Sativum* seedcake, J. Food Sci. Technol. 55 (3) (2018) 1154–1163, https://doi.org/10.1007/s13197-017-3031-8.
[59] I.F. Pérez-Ramírez, R. Reynoso-Camacho, F. Saura-Calixto, J. Pérez-Jiménez, Comprehensive characterization of extractable and nonextractable phenolic compounds by high-performance liquid chromatography–electrospray ionization–quadrupole time-of-flight of a grape/pomegranate pomace dietary supplement, J. Agric. Food Chem. 66 (3) (2018) 661–673, https://doi.org/10.1021/acs.jafc.7b05901.
[60] B.D. Arbo, C. André-Miral, R.G. Nasre-Nasser, L.E. Schimith, M.G. Santos, D. Costa-Silva, A.L. Muccillo-Baisch, M.A. Hort, Resveratrol derivatives as potential treatments for Alzheimer's and Parkinson's disease, Front. Aging Neurosci. 12 (2020), https://doi.org/10.3389/fnagi.2020.00103.
[61] M. Larrosa, J. Tomé-Carneiro, M.J. Yáñez-Gascón, D. Alcántara, M.V. Selma, D. Beltrán, M.T. García-Conesa, C. Urbán, R. Lucas, F. Tomás-Barberán, J. C. Morales, J.C. Espín, Preventive oral treatment with resveratrol pro-prodrugs drastically reduce colon inflammation in rodents, J. Med. Chem. 53 (20) (2010) 7365–7376, https://doi.org/10.1021/jm1007006.
[62] M.E.M.B. de Araújo, Y.E. Moreira Franco, T.G. Alberto, M.A. Sobreiro, M. A. Conrado, D.G. Priolli, A.C.H. Frankland Sawaya, A.L.T.G. Ruiz, J.E. de Carvalho, P. de Oliveira Carvalho, Enzymatic de-glycosylation of rutin improves its antioxidant and antiproliferative activities, Food Chem. 141 (1) (2013) 266–273, https://doi.org/10.1016/j.foodchem.2013.02.127.
[63] S.R. Alizadeh, M.A. Ebrahimzadeh, *O*-glycoside quercetin derivatives: biological activities, mechanisms of action, and structure–activity relationship for drug design, a review, Phytother. Res. 36 (2) (2022) 778–807, https://doi.org/10.1002/ptr.7352.
[64] S. Wang, Y. Chen, C. Xia, C. Yang, J. Chen, L. Hai, Y. Wu, Z. Yang, Synthesis and evaluation of glycosylated quercetin to enhance neuroprotective effects on cerebral ischemia-reperfusion, Biorg. Med. Chem. 73 (2022), 117008, https://doi.org/10.1016/j.bmc.2022.117008.
[65] A. Baldisserotto, G. Malisardi, E. Scalambra, E. Andreotti, C. Romagnoli, C. B. Vicentini, S. Manfredini, S. Vertuani, Synthesis, antioxidant and antimicrobial activity of a new phloridzin derivative for dermo-cosmetic applications, Molecules 17 (11) (2012) 13275–13289, https://doi.org/10.3390/molecules171113275.
[66] W.-T. Chang, W.-C. Huang, C.-J. Liou, Evaluation of the anti-inflammatory effects of phloretin and phlorizin in lipopolysaccharide-stimulated mouse macrophages, Food Chem. 134 (2) (2012) 972–979, https://doi.org/10.1016/j.foodchem.2012.03.002.
[67] W. Zhang, S. Chen, H. Fu, G. Shu, H. Tang, X. Zhao, Y. Chen, X. Huang, L. Zhao, L. Yin, C. Lv, J. Lin, Hypoglycemic and hypolipidemic activities of phlorizin from *Lithocarpus polystachyus* Rehd in diabetes rats, Food Science & Nutrition 9 (4) (2021) 1989–1996, https://doi.org/10.1002/fsn3.2165.
[68] E.C. Chao, R.R. Henry, SGLT2 inhibition — a novel strategy for diabetes treatment, Nat. Rev. Drug Discov. 9 (7) (2010) 551–559, https://doi.org/10.1038/nrd3180.
[69] R.P. Pandey, T.F. Li, E.-H. Kim, T. Yamaguchi, Y.I. Park, J.S. Kim, J.K. Sohng, Enzymatic synthesis of novel phloretin glucosides, Appl. Environ. Microbiol. 79 (11) (2013) 3516–3521, https://doi.org/10.1128/AEM.00409-13.
[70] T. Zhang, J. Liang, P. Wang, Y. Xu, Y. Wang, X. Wei, M. Fan, Purification and characterization of a novel phloretin-2′-*O*-glycosyltransferase favoring phloridzin biosynthesis, Sci. Rep. 6 (1) (2016) 35274, https://doi.org/10.1038/srep35274.
[71] L. Tian, J. Cao, T. Zhao, Y. Liu, A. Khan, G. Cheng, The bioavailability, extraction, biosynthesis and distribution of natural dihydrochalcone: Phloridzin, Int. J. Mol. Sci. 22 (2) (2021) 962, https://doi.org/10.3390/ijms22020962.
[72] S. Arana-Peña, D. Carballares, R. Morellon-Sterlling, Á. Berenguer-Murcia, A. R. Alcántara, R.C. Rodrigues, R. Fernandez-Lafuente, Enzyme co-immobilization: always the biocatalyst designers' choice…or not? Biotechnol. Adv. 51 (2021), 107584 https://doi.org/10.1016/j.biotechadv.2020.107584.
[73] E.T. Hwang, S. Lee, Multienzymatic cascade reactions via enzyme complex by immobilization, ACS Catal. 9 (5) (2019) 4402–4425, https://doi.org/10.1021/acscatal.8b04921.